Peer-reviewed version available at *Materials* **2017**, *10*, 136; doi:10.3390/ma10020136

Article

3D Printing of Cytocompatible Water-Based Light-Cured Polyurethane with Hyaluronic Acid for Cartilage Tissue Engineering Applications

Ming-You Shie [1,2,3], Wen-Ching Chang [1], Li-Ju Wei [1], Yu-Hsin Huang [1], Chien-Han Chen [4], Yi-Wen Chen [1,5,*], Yu-Fang Shen [1,*]

[1] 3D Printing Medical Research Center, China Medical University Hospital, China Medical University, Taichung City 40402, Taiwan; eviltacasi@gmail.com (M.-Y.S.); Jayla11218@gmail.com (W.-C.C.); lijuwei928@gmail.com (L.-J.W.); yhhuang@dragon.nchu.edu.tw (Y.-H.H.)

[2] School of Dentistry, China Medical University, Taichung City 40402, Taiwan

[3] Department of Bioinformatics and Medical Engineering, Asia University, Taichung City 41354, Taiwan

[4] School of Medicine, College of Medicine, China Medical University, Taichung 40402, Taiwan; u102001701@cmu.edu.tw

[5] Graduate Institute of Biomedical Sciences, China Medical University, Taichung City 40402, Taiwan

* Correspondence: evinchen@gmail.com (Y.-W.C.); cherryuf@gmail.com (Y.-F.S.); Tel.: +886-4-22052121 (ext. 1660) (Y.-W.C.); +886-4-22052121 (ext. 1654) (Y.-F.S.)

Abstract: Diseases in articular cartilages have affected millions of people globally. Although the biochemical and cellular composition of articular cartilages is relatively simple, there is the limitation in self-repair ability of cartilage. Therefore, developing the strategies for cartilage repair is very important. Here, we reported a new manufacturing process of water-based polyurethane based photosensitive materials with hyaluronic acid and applied the materials for 3D printed customized cartilage scaffolds. The scaffold has high cytocompatibility and is one that closely mimics the mechanical properties of articular cartilages. It is suitable for culturing human Wharton's jelly mesenchymal stem cells (hWJMSCs) and the cells showed an excellent chondrogenic differentiation capacity. We consider that the 3D

Peer-reviewed version available at Materials 2017, 10, 136; doi:10.3390/ma10020136

printing hybrid scaffolds may have potential in customized tissue engineering and facilitate the development of cartilage tissue engineering.

Keywords: water-based polyurethane; hyaluronic acid; cartilage tissue engineering; scaffold

1. Introduction

Cartilage reconstruction is an important topic in regenerative medicine [1–7]. Because of the avascularity of articular cartilage, limited proliferation of mature chondrocytes and less migration of chondrocytes surrounded by the extracellular matrix, the regeneration of articular cartilage is considered difficult in comparison to other tissue [2]. Although many approaches such as microfracture, abrasion arthroplasty, osteochondral autologous transfer and autologous chondrocyte implantation have been applied for cartilage reconstruction, there is still no ideal and perfect approach for the reconstruction of the critical articular cartilage defects and there are many problems that need to be resolved [8].

Currently, three-dimensional (3D) printing is considered as one of effective and high potential technology to revolutionize the field of regenerative medicine and tissue engineering. Previous studies also reported 3D printing is a useful method to fabricate scaffolds for cartilage tissue engineering [9,10]. In 2012, Xu *et al.* [9] used a novel multi-head deposition system to fabricate the hybrid scaffolds for cartilage tissue engineering applications. In 2014, Hung *et al.* [10] established a water-based platform technology for 3D-printed cartilage scaffold fabrication with liquid-frozen deposition manufacturing (LFDM). In 2015, Markstedt's group [11]

Peer-reviewed version available at Materials 2017, 10, 136; doi:10.3390/ma10020136

constructed 3D cartilage scaffolds with a bioink composed of nanofibrillated cellulose and alginate by electromagnetic jet technology. Although their studies demonstrated 3D printing can provide a solution for cartilage tissue engineering, the mechanical properties of the printed scaffolds were weaker than natural articular cartilage and the printing resolution should be improved.

3D printing supplies a lot of advantages for medical applications, containing high precision, fast fabrication and customized production. Many 3D printing methods including fused deposition manufacturing (FDM) [12], LFDM [13], selective laser sintering (SLS) [14], power bed and inkjet head 3D printing (PIP) [15], stereolithography (SLA) [16], and digital light processing (DLP) [17] have been applied for tissue engineering scaffold fabrication. Although FDM and LFDM technologies can provide low manufacturing cost and simple manufacturing process, the resolution is limited on a Z-axis. The problems of SLS and PIP technologies are the large amount of waste production. SLA and DLP have higher vertical resolution [18], but most light-curable polymers are dissolved in organic solvents which are low biocompatible [19]. Therefore, researchers have focused on the development of light-curable and highly biocompatible materials for SLA and DLP in recent years [20-22].

An ideal scaffold for tissue engineering is biocompatible and biodegradable and owns a desired tissue shape and porous structure for providing a nutrient and metabolic transporting pathway. DLP technology can satisfy the requirements of printing 3D scaffolds which have specific shape and porous structure, but the materials for DLP technology are the key to decide if the printed scaffolds are biocompatible and biodegradable.

Peer-reviewed version available at *Materials* **2017**, *10*, 136; doi:10.3390/ma10020136

Biodegradable materials can be gradually degraded by the biologic fluid *in vivo* or by microorganisms in the environment [23]. Previous studies reported the tissue engineering scaffolds can be fabricated by biodegradable materials including poly(ε -caprolactone) (PCL), polylactic acid (PLA), polyglycolic acid (PGA), and polylactic- co -glycolic acid (PLGA) [24]. However, the physical properties of these materials are not very similar with living tissues and some of these materials often need to be dissolved by highly toxic solvents [25,26]. Biostable polyurethanes are considered to have good biocompatibility and mechanical properties for being long term medical implants including vascular grafts and cardiac pacemakers. Polyurethanes are generally synthesized through the polycondensation reaction of diisocyanates with amines and/ alcohols [27]. In this study, the polyurethanes containing aliphatic polyesters which allow for biodegradation are applied. Besides the polyurethanes are water-based light-cured polyurethanes which could be applied in DLP technology and have good biocompatibility.

Water-based 3D printing photosensitive materials for customized cartilage tissue engineering with DLP technology is developed in this study. Water-based light-cured polyurethane is a non-toxic and environmentally friendly material, but it has not been applied in DLP technology for 3D printing yet. Here, we reported a new manufacturing process for water-based polyurethane based photosensitive materials with hyaluronic acid (HA) which has been reported to promote cartilage repair and applied the materials for 3D printed customized cartilage scaffolds. The scaffold has high biocompatibility and is one that closely mimics the mechanical properties of articular cartilages. Furthermore, it can be designed by the three-dimensional reconstruction and is similar with the shape of the cartilage defect of the

Peer-reviewed version available at Materials 2017, 10, 136; doi:10.3390/ma10020136

recipient site to provide the best effectiveness for cartilage tissue reconstruction and it will also facilitate the development of cartilage tissue engineering.

2. Results and Discussion

2.1. Fabrication of customized Scaffolds

Organic solvents such as DMF and dimethylformamide are involved in traditional PU polymerization to regulate PU viscosity to help PU coating easily. In order to substitute traditional solvent-based PU which is as volatile organic compounds (VOC), the water-based PU was developed in recent years [28]. Although water-based light-cured PU is a non-toxic and environmentally friendly material, but it was used for coating previously and wasn't applied in DLP and SLA technologies for 3D printing directly. During the curing process, the water in water-based light-cured PU resins must be removed by heat or short wave infrared. Besides, the water-based light-cured PU resins often present a solidified or over-sticky state after water removing.

The viscosity of the materials for DLP based 3D printers is a key factor and it can affect the printing resolution and printing results [29]. Here, we reported a new manufacturing process for water-based polyurethane based photosensitive materials (Figure 1A). The water-based polyurethanes were heated and stirred at high speed to remove the water, and then were added hydroxyethylmethacrylate (HEMA) to adjust the viscosity and added photoinitiators for the light curing. There is no significant difference of the Raman spectra of the water-based polyurethanes between with or without water removing processes (Figure 1B,C). Besides, the scaffolds with various shapes were fabricated by the DLP technology to confirm the printing

Peer-reviewed version available at Materials 2017, 10, 136; doi:10.3390/ma10020136

resolution and customized potential of the materials (Figure 1D). The result indicates that our materials have good printing resolution and also have great potential in customized tissue engineering.

2.2. *Characterization of Water-Based Light-Cured PU/TPU Specimens*

Water-based polyurethanes contain different types, such as water-based light-cured polyurethanes, water-based thermoplastic polyurethanes, and water-based thermosetting polyurethanes. In this study, the water-based light-cured polyurethane and the water-based thermoplastic polyurethane were mixed and heated together to remove water and to form hybrid materials. By using different proportions of the water-based light-cured PU and the water-based thermoplastic polyurethane, the hybrid specimens showed different hardness and Young's modulus (Figure 2A,B). When increasing the concentration of the water-based TPU, the hardness and Young's modulus decreased significantly. The Young's modulus of the articular cartilage according to previous studies is about 24 MPa [30]. When adding specific proportions of the water-based TPU, the physical properties of the materials were similar with articular cartilage. In addition, the cell viability of hWJMSCs cultured on the water-based polyurethane based composites with 0% or 50% of the water-based TPU for 1 and 3 days was evaluated (Figure 2C). The hWJMSCs cultured on 0 or 50% water-based thermoplastic polyurethane composites had similar or higher cell viability compared with the normal tissue culture plates (Control). In 2012, Chu *et al.* [31] also reported that the attachment and migration of WJMSCs can be promoted by PU. These results demonstrated the polyurethane based composites have high biocompatibility.

Peer-reviewed version available at Materials 2017, 10, 136; doi:10.3390/ma10020136

2.3. Characterization of Water-Based Light-Cured PU/HA Scaffolds

HA is an important component of articular cartilage. It can link aggrecan molecules to large proteoglycans and be a lubricant in joints [32]. Previous studies reported that HA can facilitate cell migration and viability [33] and may promote the chondrogenic differentiation of mesenchymal stem cells (MSCs) [34,35]. In 2016, Gobbi's group showed that HA based scaffolds with activated bone marrow–derived MSCs can provide better effects of cartilage reconstruction than microfracture and lead to successful medium-term outcomes [36]. Therefore, the HA based scaffolds with stem cells may provide great potential of the development for cartilage repair.

In this study, HA was added in the water based polyurethane composites to fabricate water-based light-cured PU/HA 3D hybrid scaffolds by DLP technology. Figure 3A shows the Raman spectra of the PU/HA hybrid scaffolds with different HA concentration. The Raman spectra of the PU/HA hybrid scaffolds with different HA concentration were very similar. When increasing the HA concentration, the height of the 1413 cm^{-1} band increased slightly. The width of the 1413 cm^{-1} band, related to the symmetrical vibration of the COO^- group of the glucuronate residue, was used to identify HA [37].

The Young's modulus and diametral tensile strength (DTS) values of the PU/HA hybrid scaffolds were shown in Figure 3B and C. The Young's modulus and DTS values had significant increases in the strength in the scaffolds with HA. We suggested that the addition of HA could react with PU to form tighter chemical structure. In addition, the Raman spectra of the PU/HA hybrid scaffolds showed that the height of the 882 cm^{-1} band of the scaffolds with HA decreased slightly compared to the scaffolds without HA (Figure 3A) and the peak at 882 cm^{-1} was attributed to C-C-O vibrations of PU.

Peer-reviewed version available at Materials 2017, 10, 136; doi:10.3390/ma10020136

These results indicated that HA may react with PU to cause the height of the 882 cm^{-1} band decreasing and to lead the scaffold strength increasing.

Figure 4A shows the degradation results of the PU/HA hybrid scaffolds for 7, 14, 21 and 28 days in phosphate buffered saline (PBS) at 37 °C. The degradation results of the all scaffolds were almost the same. All PU/HA hybrid scaffolds displayed a rapid initial weight loss in 7 days. After 28 days, the weight loss measured for all PU/HA hybrid scaffolds was about 94.5 %. Although the HA and PU containing aliphatic polyesters are biodegradable materials, the PU/HA hybrid scaffolds exhibited slow degradation rate. The Young's modulus of the PU/HA hybrid scaffolds were also evaluated after 28 days (Figure 4B). The Young's modulus of the scaffolds with HA decreased slightly after 28 days, but the Young's modulus of the scaffolds without HA increased slightly. The Figure 4C shows the images of the PU/HA hybrid scaffolds after compressing tests. The all PU/HA hybrid scaffolds without degradation tests just presented deformation after compressing, but the phenomenon of fragmentation were caused in the scaffolds containing 0-1% HA with 28-day degradation tests. It is noteworthy that the PU/HA hybrid scaffolds with 2% HA just presented the phenomenon of deformation after compressing. The SEM images of 28-day degradation tests showed that the phenomenon of the crack formation reduced gradually with the concentration of HA increasing (Figure 4D). These results indicated that the addition of HA can prevent the crack formation of the scaffolds during the degradation process and may facilitate the degradation of the scaffolds stably.

2.4. Adhesion, Proliferation and Chondrogenic Differentiation of Cells cultured on Water-Based Light-Cured PU/HA Scaffolds

The cell morphology of WJMSCs cultured on the PU/HA hybrid scaffolds

Peer-reviewed version available at Materials 2017, 10, 136; doi:10.3390/ma10020136

for 4 hours and 3 days were examined by the SEM images (Figure 5). The cells on the all PU/HA hybrid scaffolds for 4 hours displayed flat and presented intact, well-defined morphology. This result demonstrated that the cells can adhered on the scaffolds very well and the scaffolds might provide a good adhesion environment for the cells. Besides, the SEM images of the cells on the all PU/HA hybrid scaffolds for 3 days showed that the cells still presented good cell morphology and the number of cells increased. The cell proliferation of WJMSCs and chondrocytes cultured on the PU/HA hybrid scaffolds was evaluated by the PrestoBlue® assay (Figure 6). In addition, the fluorescent images showed the WJMSCs covered all the PU/HA hybrid scaffolds after 5 days incubation (Figure 7). These results indicated that the cells incubated on the PU/HA hybrid scaffolds can have good proliferation ability and the scaffolds have good biocompatibility.

In order to investigate the chondrogenic differentiation effect of the scaffolds, the fluorescent and Alcian blue staining images and the GAG contents of the micromass cultures of WJMSCs cultured on the PU/HA hybrid scaffolds for 1 day were evaluated (Figure 8A-C). The fluorescent images showed that the phenomenon of cell aggregation increased with the HA concentration increased. Besides, the color of Alcian blue staining displayed from light to deep blue and the GAG contents increased with the HA concentration increased. Furthermore, the immunofluorescence staining images (Figure 8D) showed that the WJMSCs cultured on the PU/HA hybrid scaffolds with 2% HA and without adding chondrogenic differentiation medium can express collagen type II and cartilage homeoprotein 1 (CART1) which are the markers of chondrogenic differentiation. These results indicated that the PU/HA hybrid scaffolds containing higher HA concentration might

Peer-reviewed version available at Materials 2017, 10, 136; doi:10.3390/ma10020136

stimulate chondrogenic differentiation. In 2016, Huang's group also reported that water-based polyurethane 3D printed scaffolds with HA can facilitate chondrogenic differentiation [10]. However, their scaffolds were fabricated by the LFDM technology which has the lower printing resolution. In this study, we provided a new manufacturing process of water-based polyurethane based photosensitive materials with HA for DLP technology, so the printing resolution was higher than previous study [10] and the printed 3D scaffolds can also have good biocompatibility and promote chondrogenic differentiation.

3. Materials and Methods

3.1. The Preparation of Water-Based Polyurethane Based Composites

Water-based light-cured polyurethanes and water-based thermoplastic polyurethanes were purchased from Alberdingk Boley, Germany. Different proportions of the water-based thermoplastic polyurethanes (Liquid, Solid Content 50%) were added to the water-based light-cured polyurethanes (Liquid, Solid Content 40%). The hybrid materials containing 0, 10, 20, 30, 40 or 50% water-based thermoplastic polyurethanes were heated at 130 °C and stirred at high speed for 1.5 hours to remove the water. 1.5% 2,4,6-trimethylbenzoyl-diphenyl-phosphineoxide (TPO) photoininitiators (Ciba, Switzerland) and 0, 0.5, 1 or 2% 1900 kD HA (Suvenyl; Chugai Pharmaceutical, Japan) were dissolved in HEMA (Sigma-Aldrich, U.S.A.), and then were added to the light curing waterbone polyurethane composites to mix at 70 °C for 3D printing.

3.2. Graft Fabrication

All test objects and scaffolds were designed through SolidWorks (Dassault

Peer-reviewed version available at Materials 2017, 10, 136; doi:10.3390/ma10020136

Systemes SolidWorks Corp., Waltham, MA) and fabricated by a MiiCraft high resolution home DLP 3D printer (Young Optics Inc., Hsinchu,Taiwan). The mode of fabrication was blue light digital stereolithography to cure individual 100 μm layers of at 20 s exposure. For mechanical properties of the water-based light-cured PU/TPU specimens, the samples were printed with thickness of 3 mm and a diameter of 6 mm. In addition, the water-based light-cured PU/HA scaffolds were printed with thickness of 3 mm, a diameter of 6 mm and four rectangular holes (1 mm × 1 mm × 3 mm). The uncured materials were washed off and the scaffolds were post-cured under UV light, yielding the fully cured scaffolds. The cured scaffolds were washed again for 3D cell culture.

3.3.Mechanical Properties

The hardness of the water-based polyurethane based composites was determined by the shore hardness tester. The mechanical properties were examined using an EZ-Test machine (Shimadzu, Kyoto, Japan) with a 500 N load cell at a loading rate of 1 mm/min. Young's modulus was calculated from the linear region in stress–strain curve using a theoretical model.

3.4. Raman Spectroscopy

Raman spectra were collected by a portable i-Raman system (B&W Tek , U.S.A.) with an accessional software BwRam1.1. The same spectral region chosen for the standard nor-mal variant (SNV) transformation is needed [38] with the differences of the focus depth or sample volume.

3.5. Degragation in Vitro

The degradation of the PU/HA hybrid scaffolds was examined in the PBS at 37 °C for 7, 14, 21, and 28 days. The remaining weight of the scaffolds was calculated by the following equation: remaining weight (%) = W_f / W_i × 100%

Peer-reviewed version available at Materials 2017, 10, 136; doi:10.3390/ma10020136

[39]. The W_i was the initial weight of the scaffolds. The W_f was the weight of the scaffolds which were rinsed with distilled deionized water and dried after 7-, 14-, 21-, or 28-day degradation test.

3.6. Cell Viability

Approximately 10 thousand WJMSCs and chondrocytes were directly seeded over each scaffold for 1 and 3 days. Cell cultures were maintained at 37 °C in a 5 % CO_2 atmosphere. The cell viability was determined by the PrestoBlue® (Invitrogen, Grand Island, NY) assay. The values of the absorbance were examined in a multi-well spectrophotometer (Hitachi, Tokyo, Japan) at 570 nm with a reference wavelength of 600 nm.

3.7. Cell Morphology

After 4 hours and 3 days of cell culture, the scaffolds with WJMSCs were washed with cold PBS and fixed by 1.5 % glutaraldehyde (Sigma-Aldrich, U.S.A.). After 2 hours, the scaffolds were dehydrated through a graded ethanol series for 20 min at each concentration and dried with liquid CO_2 by a critical point dryer device (LADD 28000; LADD, Williston, VT). The dried scaffolds were mounted on stubs, coated with gold particles, and examined by the Scanning electron microscopy (JEOL JSM-7401F, Tokyo, Japan).

3.8. Fluorescent Images

The stable enhanced green fluorescent protein (EGFP) WJMSCs which were established by the Retro-XTM Universal Packaging System (Clontech Laboratories Inc, U.S.A.) were cultured on the PU/HA hybrid scaffolds. After 1 and 5 days, the scaffolds with the stable cells were washed with PBS and the fluorescent images were investigated by a Zeiss Axioskop2 fluorescent microscope (Carl Zeiss, Thornwood, NY, U.S.A.).

Peer-reviewed version available at Materials 2017, 10, 136; doi:10.3390/ma10020136

3.9. Micromass Culture

The micromass culture technique was modified from Ahrens's group [40]. The cell solution of 1.6 ×10^7 viable cells/mL was prepared. 5-μL droplets of cell solution were seeded to generate micromass cultures on the scaffolds for fluorescent images, Alcian blue staining and analysis, and immunofluorescence staining.

3.10. Alcian Blue Staining and Analysis

The hWJMSCs were grown on the PU/HA hybrid scaffolds and without adding chondrogenic differentiation medium. After 24 hours, the scaffolds with hWJMSCs were fixed with 4% formaldehyde, were added sulfuric acid for 30 munities, and then were stained with 10mg/ ml Alcian blue solution for 3 hours. The Alcian blue staining images were obtained by a Zeiss Axioskop2 microscope (Carl Zeiss, Thornwood, NY, U.S.A.). Besides, the GAG -Alcian blue complexes can be dissociated and dissolved in a 4 M guanidine-HCl/ propanol mixture after staining. The values of the absorbance were examined in a multi-well spectrophotometer (Hitachi, Tokyo, Japan) at 600 nm.

3.11. Immunofluorescence Staining

The hWJMSCs were grown on the PU/HA hybrid scaffolds with 2% HA and without adding chondrogenic differentiation medium. After 24 hours, the scaffolds with hWJMSCs were fixed, and immunostained with anti-COL2A1 (rabbit), anti-CART1 (mouse), and then with anti-rabbit conjugated tetramethylrhodamine (TRITC), anti-mouse conjugated fluorescein isothiocyanate (FITC) and with 4 ´ ,6-diamidino-2-phenylindole (DAPI). Immunofluorescence images were examined by using a white light laser confocal microscope Leica TCS SP8 X (Leica Microsystems GmbH).

Peer-reviewed version available at Materials 2017, 10, 136; doi:10.3390/ma10020136

4. Conclusion

We reported that new water-based 3D printing photosensitive materials with HA applied in the development of 3D printed scaffolds for cartilage tissue engineering with DLP technology. The materials bring out the important advantages such as non-toxic, high printing resolution, good cytocompatibility and environmentally friendly. Besides, the 3D printed scaffolds can facilitate cell adhesion, proliferation and chondrogenic differentiation. Furthermore, the development can be applied for the customized cartilage tissue reconstruction (Figure 9).

Acknowledgement: We thank the Ministry of Science and Technology of Taiwan for their financial support under Grant Nos. 105-2914-I-039 -008 -A1. This study was also funded by China Medical University, Taichung, Taiwan under Grant Nos. CMU105-N-08.

Author Contributions: Ming-You Shie, Yi-Wen Chen and Yu-Fang Shen conceived and designed the experiments; Ming-You Shie, Wen-Ching Chang and Chien-Han Chen performed the experiments; Yu-Hsin Huang and Li-Ju Wei analyzed the data; Yi-Wen Chen contributed reagents/materials/analysis tools; Yu-Fang Shen and Yi-Wen Chen wrote the paper.

Conflicts of Interest: The authors declare that they have no conflict of interest.

Reference

1. Chen, J.; Wang, C.; Lu, S.; Wu, J.; Guo, X.; Duan, C.; Dong, L.; Song, Y.; Zhang, J.; Jing, D.; Wu, L.; Ding, J.; Li, D. *In vivo* chondrogenesis of adult

bone-marrow-derived autologous mesenchymal stem cells. *Cell Tissue Res.* **2005**, *319*, 429–438.

2. Newman, A. P. Articular cartilage repair. *Am. J. Sports Med.* **1998**, *26*, 309–324.

3. Malafaya, P. B.; Reis, R. L. Bilayered chitosan-based scaffolds for osteochondral tissue engineering: influence of hydroxyapatite on *in vitro* cytotoxicity and dynamic bioactivity studies in a specific double-chamber bioreactor. *Acta Biomater.* **2009**, *5*, 644–660.

4. Ge, Z.; Li, C.; Heng, B. C.; Cao, G.; Yang, Z. Functional biomaterials for cartilage regeneration. *J. Biomed. Mater. Res. A* **2012**, *100*, 2526–2536.

5. Yuan, T.; Zhang, L.; Li, K.; Fan, H.; Fan, Y.; Liang, J.; Zhang, X. Collagen hydrogel as an immunomodulatory scaffold in cartilage tissue engineering. *J. Biomed. Mater. Res. B. Appl. Biomater.* **2014**, *102*, 337–344.

6. Su, K.; Lau, T. T.; Leong, W.; Gong, Y.; Wang, D.-A. Creating a living hyaline cartilage graft free from non-cartilaginous constituents: an intermediate role of a biomaterial scaffold. *Adv. Funct. Mater.* **2012**, *22*, 972–978.

7. Li, C.; Zhang, J.; Li, Y.; Moran, S.; Khang, G.; Ge, Z. Poly (l-lactide-co-caprolactone) scaffolds enhanced with poly (beta-hydroxybutyrate-co-beta-hydroxyvalerate) microspheres for cartilage regeneration. *Biomed. Mater.* **2013**, *8*, 25005.

8. Kalson, N. S.; Gikas, P. D.; Briggs, T. W. R. Current strategies for knee cartilage repair. *Int. J. Clin. Pract.* **2010**, *64*, 1444–1452.

9. Xu, T.; Binder, K. W.; Albanna, M. Z.; Dice, D.; Zhao, W.; Yoo, J. J.; Atala, A. Hybrid printing of mechanically and biologically improved constructs for cartilage tissue engineering applications. *Biofabrication* **2013**, *5*, 15001.

10. Hung, K.-C.; Tseng, C.-S.; Hsu, S.-H. Synthesis and 3D printing of biodegradable polyurethane elastomer by a water-based process for cartilage tissue engineering applications. *Adv. Healthc. Mater.* **2014**, *3*, 1578–1587.

11. Markstedt, K.; Mantas, A.; Tournier, I.; Martinez Avila, H.; Hagg, D.; Gatenholm, P. 3D Bioprinting human chondrocytes with nanocellulose-alginate bioink for cartilage tissue engineering applications. *Biomacromolecules* **2015**, *16*, 1489–1496.

12. Ding, C.; Qiao, Z.; Jiang, W.; Li, H.; Wei, J.; Zhou, G.; Dai, K. Regeneration of a goat femoral head using a tissue-specific, biphasic scaffold fabricated with CAD/CAM technology. *Biomaterials* **2013**, *34*, 6706–6716.

13. Chien, K. B.; Makridakis, E.; Shah, R. N. Three-dimensional printing of soy protein scaffolds for tissue regeneration. *Tissue Eng. Part C. Methods* **2013**, *19*, 417–426.

14. Yeong, W. Y.; Sudarmadji, N.; Yu, H. Y.; Chua, C. K.; Leong, K. F.; Venkatraman, S. S.; Boey, Y. C. F.; Tan, L. P. Porous polycaprolactone scaffold for cardiac tissue engineering fabricated by selective laser sintering. *Acta Biomater.* **2010**, *6*, 2028–2034.

15. Sherwood, J. K.; Riley, S. L.; Palazzolo, R.; Brown, S. C.; Monkhouse, D. C.; Coates, M.; Griffith, L. G.; Landeen, L. K.; Ratcliffe, A. A three-dimensional osteochondral composite scaffold for articular cartilage repair. *Biomaterials* **2002**, *23*, 4739–4751.

16. Gauvin, R.; Chen, Y.-C.; Lee, J. W.; Soman, P.; Zorlutuna, P.; Nichol, J. W.; Bae, H.; Chen, S.; Khademhosseini, A. Microfabrication of complex porous tissue engineering scaffolds using 3D projection stereolithography. *Biomaterials* **2012**, *33*, 3824–3834.

17. Dean, D.; Wallace, J.; Siblani, A.; Wang, M. O.; Kim, K.; Mikos, A. G.; Fisher, J. P. Continuous digital light processing (cDLP): highly accurate additive manufacturing of tissue engineered bone scaffolds. *Virtual Phys. Prototyp.* **2012**, *7*, 13–24.

18. Choi, J.-W.; Wicker, R.; Lee, S.-H.; Choi, K.-H.; Ha, C.-S.; Chung, I. Fabrication of 3D biocompatible/biodegradable micro-scaffolds using dynamic mask projection microstereolithography. *J. Mater. Process. Technol.* **2009**, *209*, 5494–5503.

19. Chia, H. N.; Wu, B. M. Recent advances in 3D printing of biomaterials. *J. Biol. Eng.* **2015**, *9*, 4.

20. Elomaa, L.; Teixeira, S.; Hakala, R.; Korhonen, H.; Grijpma, D. W.; Seppälä, J. V Preparation of poly(ε-caprolactone)-based tissue engineering scaffolds by stereolithography. *Acta Biomater.* **2011**, *7*, 3850–3856.

21. Melchels, F. P. W.; Feijen, J.; Grijpma, D. W. A poly(d,l-lactide) resin for the preparation of tissue engineering scaffolds by stereolithography. *Biomaterials* **2009**, *30*, 3801–3809.

22. Seck, T. M.; Melchels, F. P. W.; Feijen, J.; Grijpma, D. W. Designed biodegradable hydrogel structures prepared by stereolithography using poly(ethylene glycol)/poly(d,l-lactide)-based resins. *J. Control. Release* **2010**, *148*, 34–41.

23. Eglin, D.; Alini, M. Degradable polymeric materials for osteosynthesis: tutorial. *Eur. Cell. Mater.* **2008**, *16*, 80–91.

24. Nair, L. S.; Laurencin, C. T. Biodegradable polymers as biomaterials. *Prog. Polym. Sci.* **2007**, *32*, 762–798.

25. Gunatillake, P. A.; Adhikari, R. Biodegradable synthetic polymers for tissue engineering. *Eur. Cell. Mater.* **2003**, *5*, 1–16; discussion 16.

26. Sohier, J.; Moroni, L.; van Blitterswijk, C.; de Groot, K.; Bezemer, J. M. Critical factors in the design of growth factor releasing scaffolds for cartilage tissue engineering. *Expert Opin. Drug Deliv.* **2008**, *5*, 543–566.

27. Szycher, M. *Scycher's handbook of polyurethanes*; CRC Press: Boca Raton, FL, 1999.

28. Wang, Z.; Wan, P.; Ding, M.; Yi, X.; Li, J.; Fu, Q.; Tan, H. Synthesis and micellization of new biodegradable phosphorylcholine-capped polyurethane. *J. Polym. Sci. Part A Polym. Chem.* **2011**, *49*, 2033–2042.

29. Stampfl, J.; Wöß, A.; Seidler, S.; Fouad, H.; Pisaipan, A.; Schwager, F.; Liska, R. Water soluble, photocurable resins for rapid prototyping applications. *Macromol. Symp.* **2004**, *217*, 99–108.

30. J.R. Claycomb; Tran, J. Q. P. *Introductory Biophysics: Perspectives on the Living State*; Jones & Bartlett Learning, 2010.

31. Huang, C.; Chu, M.; Lin, C.; Chen, H.; Hung, H.; Sun, W.; Kao, W.; Hsu, S. Enhanced migration of Wharton ' s Jelly mesenchymal stem cells grown on polyurethane nanocomposites. *33*, 139–148.

32. Rutjes, A. W. S.; Juni, P.; da Costa, B. R.; Trelle, S.; Nuesch, E.; Reichenbach, S. Viscosupplementation for osteoarthritis of the knee: a systematic review and meta-analysis. *Ann. Intern. Med.* **2012**, *157*, 180–191.

33. Filardo, G.; Kon, E.; Roffi, A.; Di Martino, A.; Marcacci, M. Scaffold-based repair for cartilage healing: a systematic review and technical note. *Arthroscopy* **2013**, *29*, 174–186.

34. Kujawa, M. J.; Caplan, A. I. Hyaluronic acid bonded to cell-culture surfaces stimulates chondrogenesis in stage 24 limb mesenchyme cell cultures. *Dev. Biol.* **1986**, *114*, 504–518.

35. Kim, I. L.; Mauck, R. L.; Burdick, J. A. Hydrogel design for cartilage tissue engineering: a case study with hyaluronic acid. *Biomaterials* **2011**, *32*, 8771–8782.

36. Gobbi, A.; Whyte, G. P. One-stage cartilage repair using a hyaluronic acid–based scaffold with activated bone marrow–derived mesenchymal stem cells compared with microfracture: five-year follow-up . *Am. J. Sport. Med.* **2016**, *44* , 2846–2854.

37. Bansil, R.; Yannas, I. V; Stanley, H. E. Raman spectroscopy: a structural probe of glycosaminoglycans. *Biochim. Biophys. Acta* **1978**, *541*, 535–542.

38. Afseth, N. K.; Segtnan, V. H.; Wold, J. P. Raman spectra of biological samples: A study of preprocessing methods. *Appl. Spectrosc.* **2006**, *60*, 1358–1367.

39. Fu, S.; Ni, P.; Wang, B.; Chu, B.; Peng, J.; Zheng, L.; Zhao, X.; Luo, F.; Wei, Y.; Qian, Z. *In vivo* biocompatibility and osteogenesis of electrospun poly(epsilon-caprolactone)-poly(ethylene glycol)-poly(epsilon-caprolactone)/nano-hydroxyapatite composite scaffold. *Biomaterials* **2012**, *33*, 8363–8371.

40. Ahrens, P. B.; Solursh, M.; Reiter, R. S. Stage-related capacity for limb chondrogenesis in cell culture. *Dev. Biol.* **1977**, *60*, 69–82.

Peer-reviewed version available at Materials 2017, 10, 136; doi:10.3390/ma10020136

Figure Legends

Figure 1. (A) The schematics of the manufacturing process of the water-based polyurethane based photosensitive materials. The Raman spectra of the (B) water-based light-cured polyurethanes and (C) water-based thermoplastic polyurethanes with or without water removing processes. (D) The images of the printed scaffolds.

Figure 2. The physical properties and cell viability of the water-based polyurethane based photosensitive materials with different proportions of the water-based thermoplastic polyurethane. (A) Shore hardness values and (B) Young's modulus of the water-based polyurethane based composites compared with articular cartilage. (C) Cell viability of hWJMSCs cultured on the water-based polyurethane based composites with 0% or 50% of the water-based thermoplastic polyurethane for 1 and 3 days. Values in (A), (B) and (C) represent mean and SD (n = 3).

Figure 3. (A) Raman spectra of the PU/HA hybrid scaffolds with different HA concentration. The (B) Young's modulus and (C) diametral tensile strength values of the PU/HA hybrid scaffolds.

Figure 4. The mechanical properties and degradation rate of the PU/HA hybrid scaffolds. (A) The degradation profile of the PU/HA hybrid scaffolds with different HA concentration, expressed as the percent remaining weight. The (B) Young's modulus and (C) images of the PU/HA hybrid scaffolds after compressing tests for 0-and 28-day degradation tests. (D) The SEM images of the PU/HA hybrid scaffolds after 28-day degradation tests. The scale bar is 1 mm.

Figure 5. The SEM micrographs of hWJMSCs cultured on the PU/HA hybrid scaffolds with different HA concentration for (A) 4 hours and (B) 3 days.

Peer-reviewed version available at Materials 2017, 10, 136; doi:10.3390/ma10020136

Figure 6. The cell proliferation of WJMSCs and chondrocytes cultured on the PU/HA hybrid scaffolds for 24 and 48 hours.

Figure 7. The fluorescent images of hWJMSCs cultured on the PU/HA hybrid scaffolds for 1 and 5 days.

Figure 8. The (A) fluorescent and (B) Alcian blue staining images and the (C) GAG contents of the micromass cultures of WJMSCs cultured on the PU/HA hybrid scaffolds for 1 day. (D) The immunofluorescence staining images of nuclei (blue), COL2A1 (red) and CART1 (green) for the micromass cultures of WJMSCs cultured on the PU/HA hybrid scaffolds with 2% HA for 1 day.

Figure 9. Schematic elucidating the process of customizing cartilage tissue for cartilage repair. First, the computerized tomographic (CT) images are used for three-dimensional reconstruction. The customized porous scaffolds which are similar with the shape of the cartilage defect of the recipient site are printed with the water-based light-cured PU/HA hybrid materials by DLP technology. Furthermore, the printed PU/HA hybrid scaffolds with cultured cells are applied for cartilage repair.

Peer-reviewed version available at Materials 2017, 10, 136; doi:10.3390/ma10020136

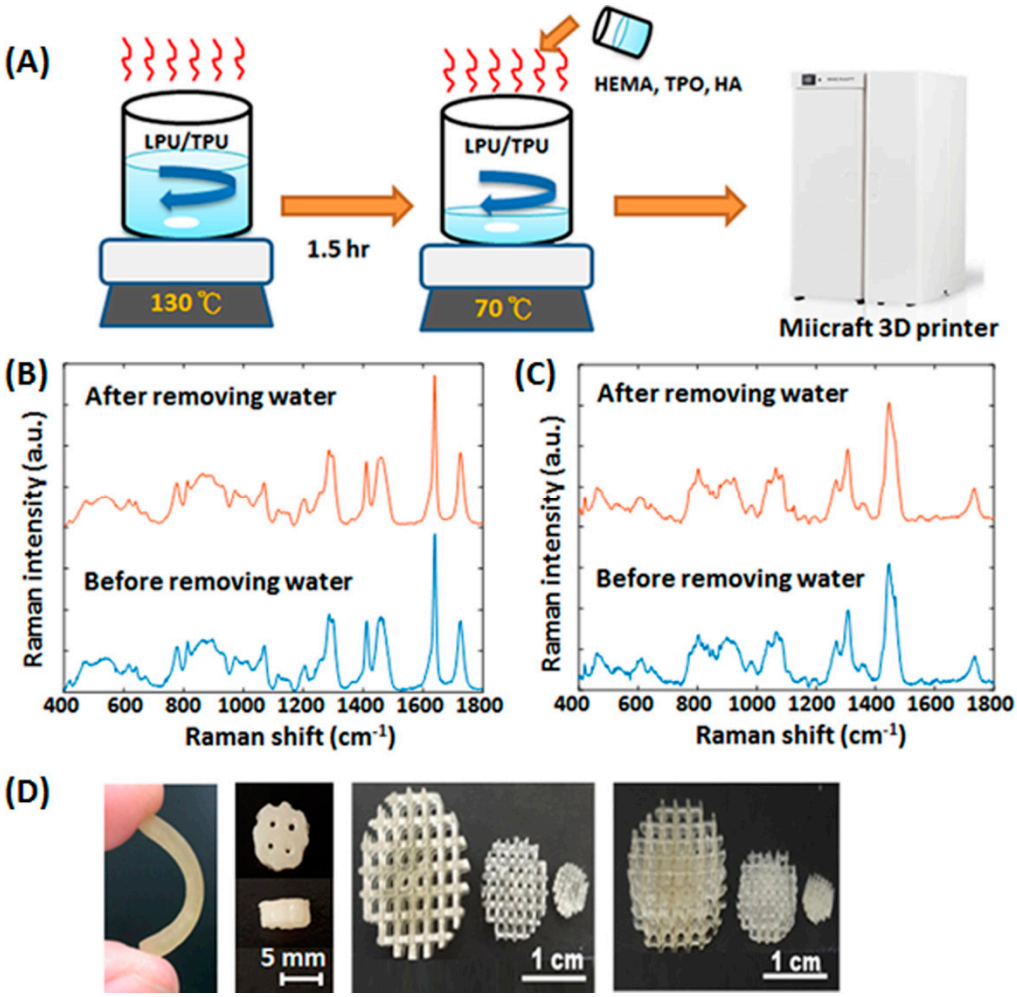

Figure 1

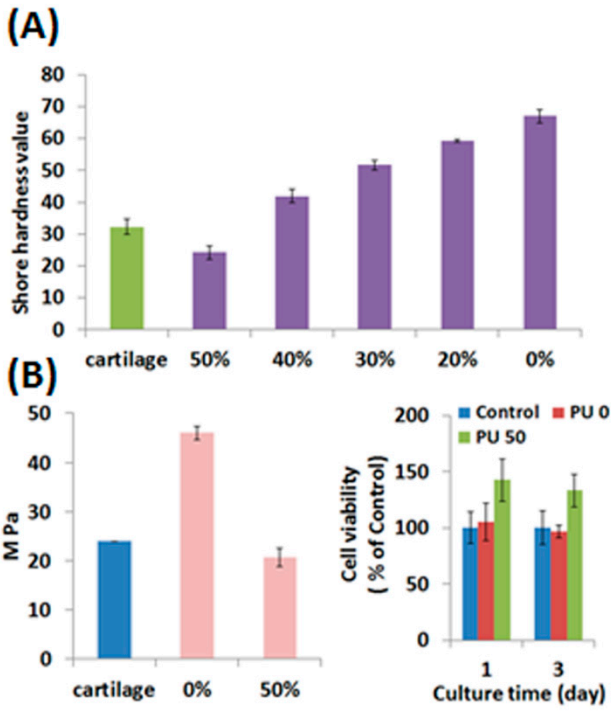

Figure 2

Peer-reviewed version available at Materials 2017, 10, 136; doi:10.3390/ma10020136

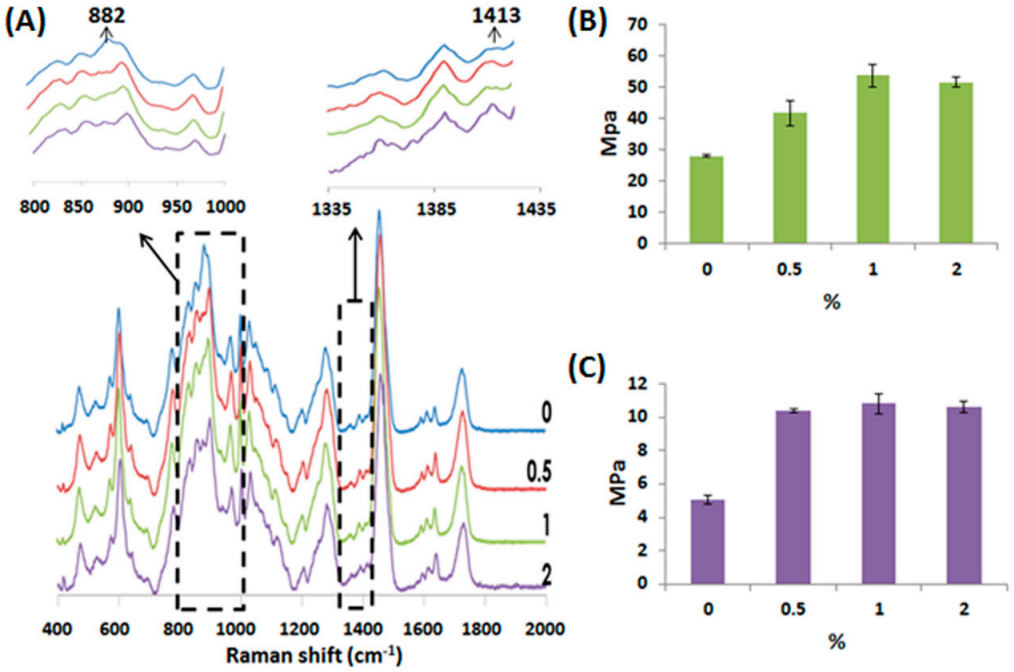

Figure 3

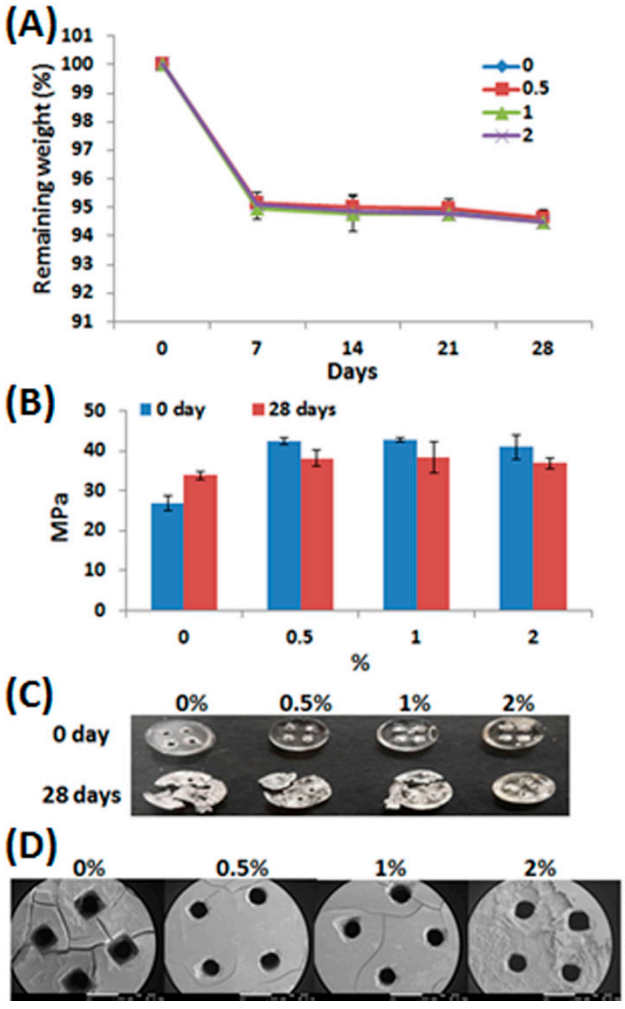

Figure 4

Peer-reviewed version available at Materials 2017, 10, 136; doi:10.3390/ma10020136

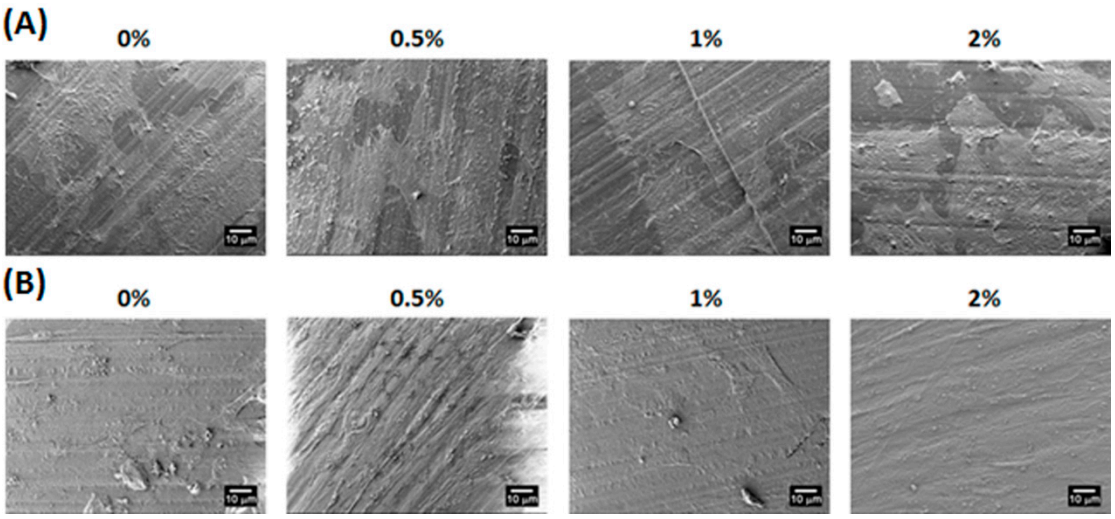

Figure 5

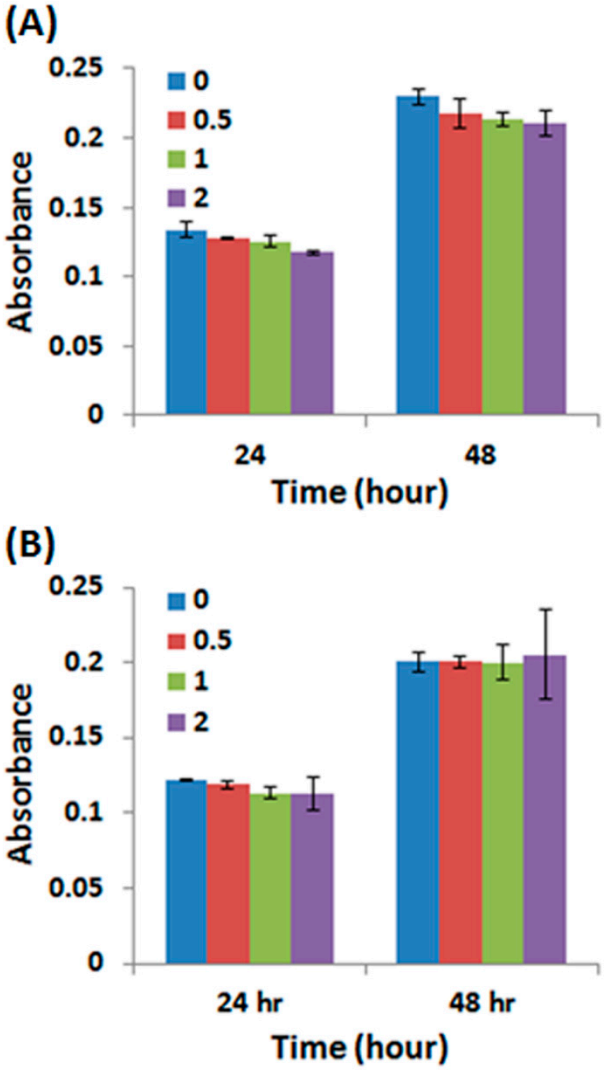

Figure 6

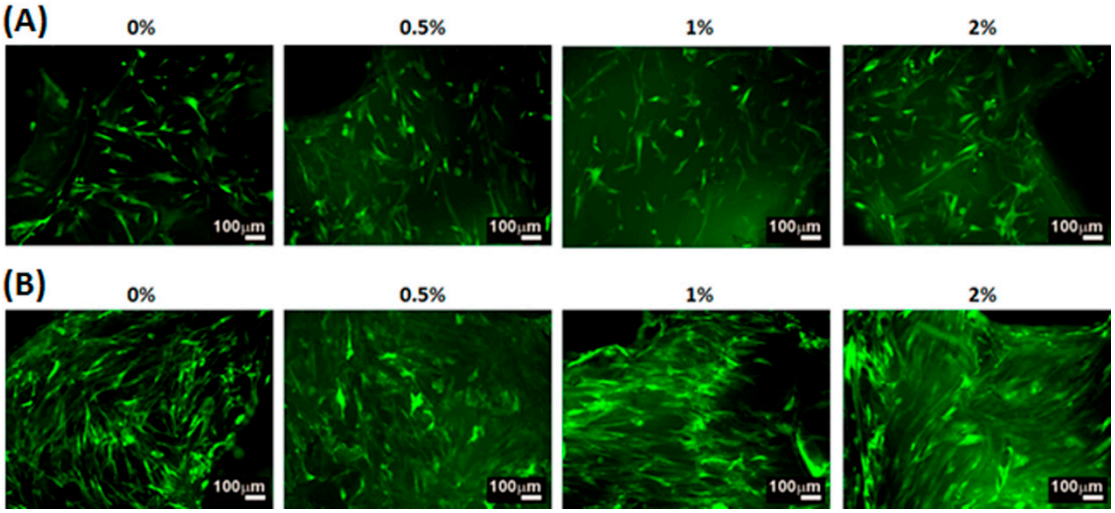

Figure 7

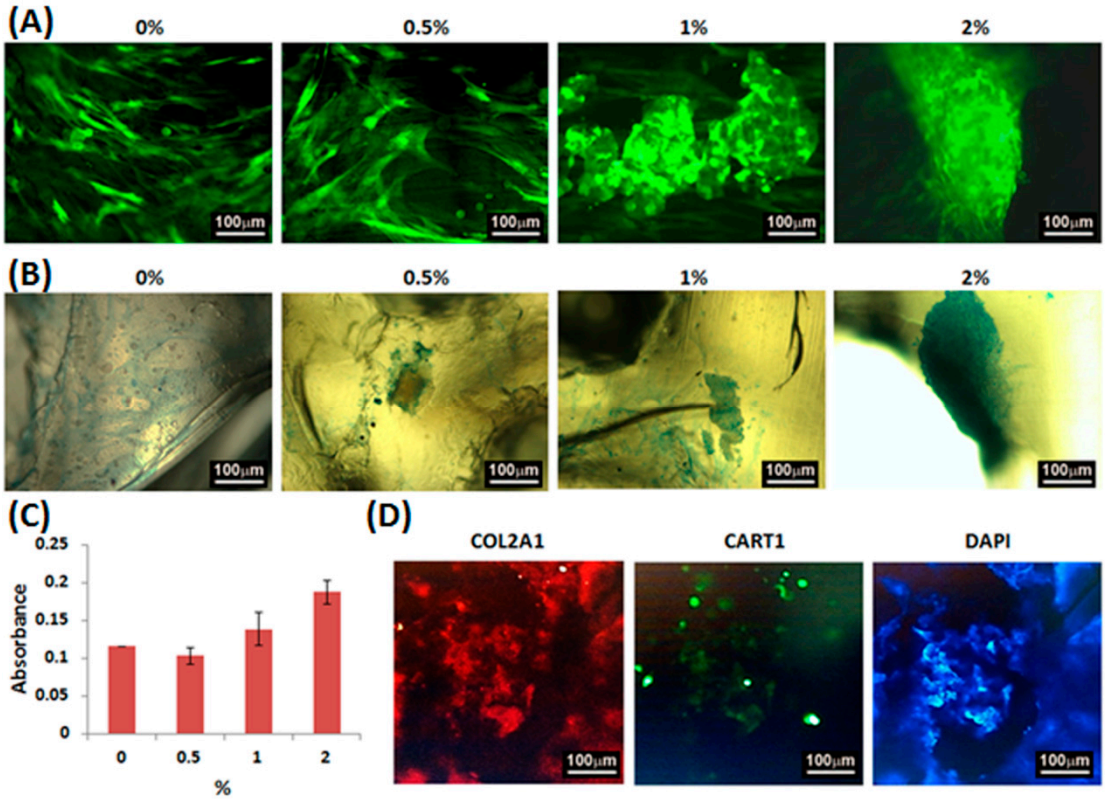

Figure 8

Peer-reviewed version available at *Materials* **2017**, *10*, 136; doi:10.3390/ma10020136

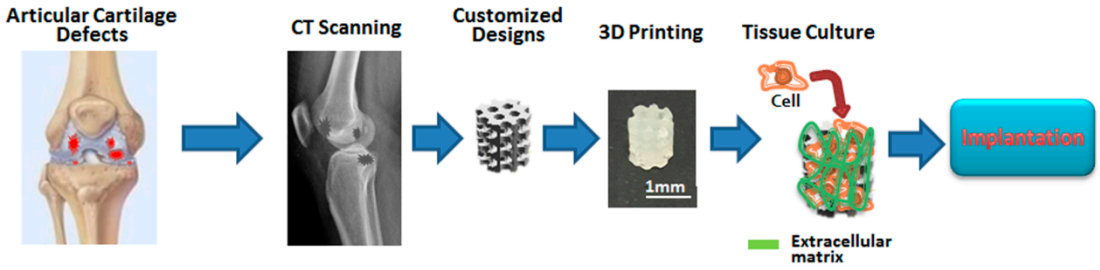

Figure 9